Temperature-calibrated high-precision refractometer using a tilted fiber Bragg grating

BIQIANG JIANG,[1,2,*], KAIMING ZHOU,[2,3] CHANGLE WANG,[2] YUNHE ZHAO,[2] JIANLIN ZHAO,[1] AND LIN ZHANG[2,4]

[1]*MOE Key Laboratory of Material Physics and Chemistry under Extraordinary Conditions and Shaanxi Key Laboratory of Optical Information Technology, School of Science, Northwestern Polytechnical University, Xi'an 710072, China*
[2]*Aston Institute of Photonic Technologies, Aston University, Birmingham B4 7ET, United Kingdom*
[3]*State Key Laboratory of Transient Optics and Photonics, Xi'an Institute of Optics and Precision Mechanics, Chinese Academy of Sciences, Xi'an 710119, China*
[4]*l.zhang@aston.ac.uk*
**bqjiang@nwpu.edu.cn*

Abstract: We present a refractometer with main- and vernier-scale to measure the refractive index (RI) of liquids with high precision by using the fine spectrum structure of a tilted fiber Bragg grating (TFBG). The absolute RI values are determined by the accurate wavelength of cut-off mode resonances. The main- and vernier-scale are calibrated by measuring large groups of fine spectra at different cut-off mode resonances in a small RI range, and the use of vernier-scale certainly reduces the RI measurement uncertainty resulted from the discrete cladding mode resonances. The performance of the TFBG-based vernier refractometer is experimentally verified by exploring the temperature dependence of RI of anhydrous ethanol in a near infrared region, showing an enhanced accuracy to the order of 10^{-4}, high repeatability and temperature self-calibration capability.

OCIS codes: (060.2340) Fiber optics components; (060.3735) Fiber Bragg gratings; (060.2370) Fiber optics sensors.

References and links

1. S. Kedenburg, M. Vieweg, T. Gissibl, and H. Giessen, "Linear refractive index and absorption measurements of nonlinear optical liquids in the visible and near-infrared spectral region," Opt. Mater. Express **2**(11), 1588-1611 (2012).
2. W. Chen, J. E. Saunders, J. A. Barnes, S. S. H. Yam, and H.-P. Loock, "Monitoring of vapor uptake by refractive index and thickness measurements in thin films," Opt. Lett. **38**(3), 365-367 (2013).
3. J. E. Saunders, H. Chen, C. Brauer, M. Clayton, W. Chen, J. A. Barnes, and H.-P. Loock, "Quantitative diffusion and swelling kinetic measurements using large-angle interferometric refractometry," Soft Matter **11**(45), 8746-8757 (2015).
4. C. Caucheteur, T. Guo, F. Liu, B.-O. Guan, and J. Albert, "Ultrasensitive plasmonic sensing in air using optical fibre spectral combs," Nat. Commun. **7**13371 (2016).
5. K. Zhou, L. Zhang, X. Chen, and I. Bennion, "Low thermal sensitivity grating devices based on Ex-45° tilting structure capable of forward-propagating cladding modes coupling," J. Lightwave Technol. **24**(12), 5087-5094 (2006).
6. Z. Yan, Z. Sun, K. Zhou, B. Luo, J. Li, H. Wang, Y. Wang, W. Zhao, and L. Zhang, "Numerical and experimental analysis of sensitivity-enhanced RI sensor based on Ex-TFG in thin cladding fiber," J. Lightwave Technol. **33**(14), 3023-3027 (2015).
7. B. Jiang, X. Lu, X. Gan, M. Qi, Y. Wang, L. Han, D. Mao, W. Zhang, Z. Ren, and J. Zhao, "Graphene-coated tilted fiber-Bragg grating for enhanced sensing in low-refractive-index region," Opt. Lett. **40**(17), 3994-3997 (2015).
8. W. Jin, Y. Cao, F. Yang, and H. L. Ho, "Ultra-sensitive all-fibre photothermal spectroscopy with large dynamic range," Nat. Commun. **6**6767 (2015).
9. Q. Wu, Y. Semenova, P. Wang, and G. Farrell, "High sensitivity SMS fiber structure based refractometer – analysis and experiment," Opt. Express **19**(9), 7937-7944 (2011).
10. A. Iadicicco, A. Cusano, S. Campopiano, A. Cutolo, and M. Giordano, "Thinned fiber Bragg gratings as refractive index sensors," IEEE Sensors Journal **5**(6), 1288-1295 (2005).
11. C. Guan, X. Tian, S. Li, X. Zhong, J. Shi, and L. Yuan, "Long period fiber grating and high sensitivity refractive index sensor based on hollow eccentric optical fiber," Sens. Actuators B Chem. **188**768-771 (2013).

12. J. Albert, L.-Y. Shao, and C. Caucheteur, "Tilted fiber Bragg grating sensors," Laser Photonics Rev. **7**(1), 83-108 (2013).
13. G. Laffont, and P. Ferdinand, "Tilted short-period fibre-Bragg-grating-induced coupling to cladding modes for accurate refractometry," Meas. Sci. Technol. **12**(7), 765-770 (2001).
14. B. Jiang, J. Zhao, C. Qin, W. Jiang, A. Rauf, F. Fan, and Z. Huang, "Method for measuring liquid phase diffusion based on tilted fiber Bragg grating," Opt. Lett. **36**(21), 4308-4310 (2011).
15. C. Chan, C. Chen, A. Jafari, A. Laronche, D. J. Thomson, and J. Albert, "Optical fiber refractometer using narrowband cladding-mode resonance shifts," Appl. Opt. **46**(7), 1142-1149 (2007).
16. T. Guo, C. Chen, A. Laronche, and J. Albert, "Power-referenced and temperature-calibrated optical fiber refractometer," IEEE Photon. Technol. Lett. **20**(8), 635-637 (2008).
17. B. Jiang, J. Zhao, Z. Huang, A. Rauf, and C. Qin, "Real-time monitoring the change process of liquid concentration using tilted fiber Bragg grating," Opt. Express **20**(14), 15347-15352 (2012).
18. W. Zhou, D. J. Mandia, S. T. Barry, and J. Albert, "Absolute near-infrared refractometry with a calibrated tilted fiber Bragg grating," Opt. Lett. **40**(8), 1713-1716 (2015).
19. W. Zhou, Y. Zhou, and J. Albert, "A true fiber optic refractometer," Laser Photonics Rev. **11**(1), 1600157 (2017).
20. T. Guo, F. Liu, Y. Liu, N.-K. Chen, B.-O. Guan, and J. Albert, "In-situ detection of density alteration in non-physiological cells with polarimetric tilted fiber grating sensors," Biosens. Bioelectron. **55**452-458 (2014).
21. B. Jiang, X. Lu, D. Mao, W. Zhang, and J. Zhao, "*In-Situ* monitoring method for solution volatilization using tilted fiber Bragg grating," IEEE Sens. J. **15**(5), 3000-3003 (2015).
22. I. H. Malitson, "Interspecimen comparison of the refractive index of fused silica," J. Opt. Soc. Am. **55**(10), 1205-1209 (1965).
23. M. N. Polyanskiy, "Refractive index database (Fused silica)," https://refractiveindex.info/?shelf=glass&book=fused_silica&page=Malitson.
24. W. Qian, C.-L. Zhao, S. He, X. Dong, S. Zhang, Z. Zhang, S. Jin, J. Guo, and H. Wei, "High-sensitivity temperature sensor based on an alcohol-filled photonic crystal fiber loop mirror," Opt. Lett. **36**(9), 1548-1550 (2011).
25. J. E. Saunders, C. Sanders, H. Chen, and H.-P. Loock, "Refractive indices of common solvents and solutions at 1550nm," Appl. Opt. **55**(4), 947-953 (2016).

1. Introduction

The refractive index (RI) is an important physical property to be measured in laboratories and field tests, and it can be obtained with a refractometer. Abbe refractometers based on Snell's law have been mostly used through measurement of the critical angle of total reflection, which is dependent on the known, relatively high RI of a glass prism and the RI of the sample to be tested [1-3]. As a result, the Abbe refractometer can measure the absolute RI without a reference. Fiber optic-based approaches offer advantageous remote, *in-situ*, and distributed measurement of surrounding RI, and a lot of research efforts employing fiber gratings and interferometers [4-11] are being developed for compact, cost-effective, and high-accuracy RI measurement. Among them based on fiber gratings, tilted fiber Bragg gratings (TFBGs) have demonstrated outstanding performance in high-sensitivity RI measurement by taking advantages of well-established FBG technology and resonant excitations of cladding modes [12]. With increasing of the surrounding RI, some of the resonant cladding modes will gradually escape confinement of the fiber cladding, evolving into the leaky modes, and there is a "cut-off" mode resonance between the leaky modes and guided cladding modes. Utilizing different spectral features of a TFBG with regards to the surrounding RI, several methods have been developed to measure the RIs of liquid samples: i) the envelope area of the cladding mode spectrum [13, 14]; ii) the wavelengths of cladding modes [15]; iii) the transmission or reflection power [16, 17]; iv) the wavelength of cut-off mode [18, 19], which can be regarded as a "true" refractometer and achieve the absolute measurement of RI, completely analogous to an Abbe refractometer. However, the above mentioned four methods have their drawbacks. Method i) involves more spectrum processing including peak extraction and calculation of normalized area, for ii), there is a smaller wavelength shift (or lower sensitivity) in low RI region for a specific cladding mode, for iii) the measurement is more susceptible to power fluctuation caused by bend or other environmental disturbance, and for iv) only discrete cut-off wavelengths can be read, leading to a non-continuous RI measurement and a larger measurement uncertainty [18]. Apart from the above methods, by

tracking the wavelength or amplitude of a selected cut-off or adjacent mode, higher accuracy RI measurement has been reported on the investigation of the dispersion of pure water [19] and the discrimination of bio-samples with low concentrations [20], and both involved a very small RI range and cannot be applied to a relatively large range measurement.

In the work reported here, we introduce a new concept TFBG based on refractometer which has main- and vernier- scale capable of RI measurement of high precision and large dynamic range. The order of the cut-off mode is utilized as the main-scale for coarse measurement, and the much finer spectral shift at different cut-off modes are used as "vernier-scale" for high-precision RI measurement. Meanwhile, since the temperature has great influence on the RI value of materials, the desirable immunity to temperature interference in practical applications can be achieved with the help of the remaining Bragg resonance calibration of the TFBG. To validate the proposed scheme, the temperature dependence of RI of anhydrous ethanol was explored. A small continuous RI change of ethanol in the temperature range of 20°C ~ 50°C has led to a covering of a few cut-off mode resonances, and more accurate RI and temperature measurement are simultaneously presented.

2. Principle

Figure 1(a) depicts a schematic diagram of a TFBG structure for RI measurement. It is well known that the tilted fringes of a grating can enhance the light coupling from the forward-propagating core mode to backward-propagating cladding modes at shorter wavelengths, and simultaneously reduce the coupling of the backward-propagating core mode. The resonances between the backward coupled core (λ_{co}) and cladding (λ_{cl}) modes of the TFBG are determined by the phase-matching conditions

$$\lambda_{co} = 2n_{eff}^{co}\left(\lambda_{co}\right)\Lambda_g , \tag{1}$$

$$\lambda_{cl} = \left[n_{eff}^{co}\left(\lambda_{cl}\right) + n_{eff}^{cl}\left(\lambda_{cl}\right)\right]\Lambda_g , \tag{2}$$

where, $n_{eff}^{co}\left(\lambda_{co}\right)$ and $n_{eff}^{co}\left(\lambda_{cl}\right)$ are the ERIs of the core mode at the wavelengths of λ_{co} and λ_{cl}, respectively, $n_{eff}^{cl}\left(\lambda_{cl}\right)$ is the ERI of the cladding mode at λ_{cl}, and the Λ_g is the actual grating period along the fiber axis. By using Eqs. (1) and (2), in combination with the known dispersion of the core mode, i.e. $n_{eff}^{co}\left(\lambda_{co}\right)$, $n_{eff}^{co}\left(\lambda_{cl}\right)$, the surrounding RI can be calculated by the measurement of cladding resonant wavelength λ_{cl} and the Bragg wavelength λ_{co}. Any change of the surrounding RI will result in the shift of λ_{cl} while the core resonance at λ_{co} remains unchanged. However, variation of temperature and strain to the grating will produce spectral shifts for both λ_{cl} and λ_{co}.

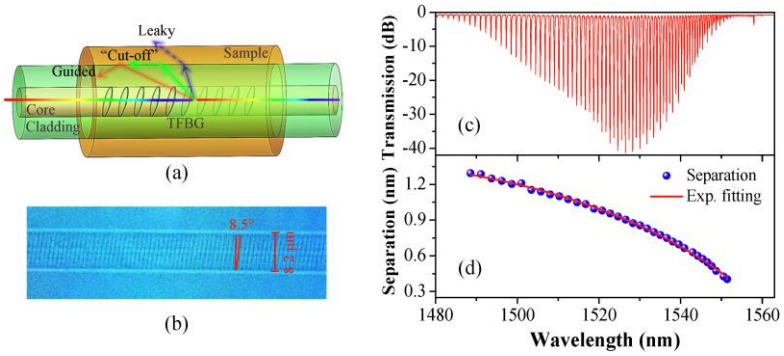

Fig. 1. (a) Schematic model of a TFBG-based refractometer, (b) optical microscopic image of tilted fringes of an 8.5° TFBG, (c) transmission spectra of the TFBG, and (d) separations of adjacent cladding mode resonances at different mode-orders or resonant wavelengths.

As depicted in Fig. 1(a), when the ERI of a cladding mode becomes lower than the RI of the sample to-be measured, the cladding mode will be no longer confined in the fiber cladding, and then degrade into a leaky mode propagating in the surrounding medium. On the other hand, modes with ERI higher than the surrounding RI are totally confined within the cladding boundary, and the mode with ERI equal to the surrounding RI is regarded as a "cut-off" cladding mode, analogous to the critical angle of an Abbe refractometer [18]. The surrounding RI can thus be determined from Eqs. (1) - (2) and tracking the wavelength of the cut-off cladding mode. Existing reports used resonant wavelength of the cut-off mode to determine surrounding RI, which presented step values because of discreteness of the cladding mode resonances, leading to a considerable measurement uncertainty.

However, it is noted that a small variation of surrounding RI will not change the order of cut-off cladding mode but cause a wavelength shift. To improve the measurement accuracy of RI, the variation of fine spectra of each cut-off mode resonance in a small RI range can be utilized as vernier scale for precise RI/ERI calibration.

3. Device fabrication, experimental results and discussion

3.1 Fabrication of tilted fiber Bragg grating based refractometer

In the experiment, the employed TFBG was UV-inscribed in hydrogenated standard SMF-28 with a frequency doubled continuous wave argon-ion laser (244nm) using the scanning phase-mask technique. The tilted structure was realized by rotating the phase-mask in the fabrication system. The fabricated TFBG was annealed at 80°C for 48 hours to release the residual hydrogen and stabilize the grating structure. The length and the internal tilt angle were 12mm and 8.5° to excite strong cladding mode resonances for measurement of liquid-sample. With a period of 1066.39nm for the uniform phase-mask, the axial grating period Λ_g is 539.84 nm for tilt angle of 8.5°. Figure 1(b) shows the tilted fringes in the fiber core of the TFBG inspected with a high resolution microscope. The corresponding spectrum of the TFBG is shown in Fig.1(c). And the operating range of the RI sensor can be adjusted by the tilt angle for better quality factor for the measurement signal and different measurement ranges of RI measurement. The separation between the adjacent resonances changes with the mode order, as shown in Fig. 1(d). Clearly, the higher-order cladding modes at the shorter wavelength side demonstrate a larger separation.

3.2 Identification of main-scale of the refractometer

The RI response of the TFBG was examined by using an experimental system as described in [21], including a supercontinuum light source, sample cell and optical spectrum analyzer (OSA). In the experimental process, the broadband light signal from the light source is coupled in the TFBG, and the transmission signal is monitored and recorded by the OSA. A series of RI matching liquids (from Cargille Labs) ranging from 1.3200 to 1.4500 with an interval of 0.005 (with maximum error of 0.0002 standardized at 589.3 nm and 25°C) were injected into the sample cell in turn and used as calibration samples to change the RI around the TFBG. The measured spectra of TFBG for various RI values are demonstrated in Fig. 2(a), and the position of cut-off mode resonance for each RI is indicated in the shadow area. The so-called "cut-off" mode is located between the leaky and guided modes, as clearly shown in the inset of Fig. 2(a), which is evidenced by an apparent reduction of coupling intensity compared with the guided cladding mode at the longer wavelength side.

The extracted wavelengths of cut-off mode resonances at each RI are shown in Fig. 2(b). From the measurement result, the slope of RI response curve of the TFBG is 508.681 nm/RIU ("RIU" represents the refractive index unit). However, the discretization in the wavelength extraction of cut-off cladding modes introduce a RI measurement uncertainty of $\pm 1.2\times10^{-3}$, which means any small RI change in this range cannot be precisely detected. Also, this uncertainty is dependent on the wavelength separation between adjacent cut-off cladding

modes, and there will be a larger measurement error for the lower RI region corresponding to the higher-order mode, where biochemical sensing interests in.

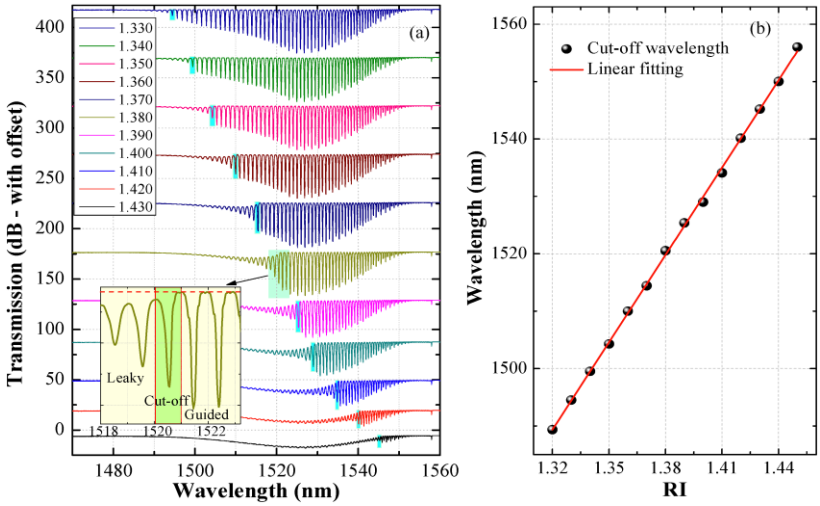

Fig. 2. (a) Spectral evolution of TFBG-1 with the RI change. The cut-off mode position for each RI value is shown in the shadow area. The inset is the zoomed spectrum of the cut-off mode resonance for RI of 1.380. (b) Wavelengths of cut-off mode resonances of the TFBG versus surrounding RI.

3.3 Calibration for "vernier-scale" of the refractometer

To improve the measurement accuracy, it is essential that a more precise measuring scale with smaller steps is required to fill in the gap between the discrete cut-off cladding modes. As mentioned above, a small variation of RI will not change the order of cut-off mode but affect its absolute wavelength position. Therefore, we prepared a series of sucrose solutions with different concentrations from 0% (DI water) to 50% for fine measurement. Continuously tiny change of concentration and thus RI can be attained by volatilization of water in solution. The RIs of these sucrose solutions were coarsely pre-calibrated with an Abbe refractometer and calculated in terms of cut-off wavelength. Owing to the slow volatilization at room temperature, the concentration (or RI) of sucrose solution can be assumed to a linear change in a very small range, in which the order of cut-off mode resonance can transfer to next one. And then, with the change of surrounding RI, we obtained large groups of finer (or defined as "vernier") spectra at different cut-off modes, as shown in Fig. 3.

Analogous to that of a vernier caliper, metering using a TFBG-based refractometer can be done with a main-scale and a "vernier-scale". But here, the main- and vernier-scale correspond to the coarse wavelengths (or orders) of cut-off modes (marked in the top-left inset of Fig. 3(a)), and finer spectral shift (zoomed region in the bottom-right inset of Fig. 3(a)) of each cut-off mode, respectively. They have different response coefficients to the RI. Therefore, the RI value can be obtained from the calibration curve of not only main-scale, but also more precise vernier-scale. From the spectral evolutions at two different cut-off mode resonances shown in Fig. 3(b), the cut-off mode is identified, and in a small RI range, this resonance is noticeably going toward longer wavelength and lower coupling intensity, while the leaky mode to the left and the last guided mode to the right show a shrinkage of coupling intensity and an ambiguous wavelength shift, respectively. Moreover, by substituting Eq. (1) into Eq. (2), the ERI of the cladding mode can be calculated at the wavelength λ_{cl} as follows

$$n_{\mathrm{eff}}^{\mathrm{cl}}\left(\lambda_{\mathrm{cl}}\right)=\frac{2\lambda_{\mathrm{cl}}}{\lambda_{\mathrm{co}}}n_{\mathrm{eff}}^{\mathrm{co}}\left(\lambda_{\mathrm{co}}\right)-n_{\mathrm{eff}}^{\mathrm{co}}\left(\lambda_{\mathrm{cl}}\right). \tag{3}$$

Where, the ERIs $n_{\text{eff}}^{\text{co}}\left(\lambda_{\text{co}}\right)$ and $n_{\text{eff}}^{\text{co}}\left(\lambda_{\text{cl}}\right)$ of the core mode at the two resonant wavelengths of λ_{co} and λ_{cl} are obtained by means of Eq. (1) and the core RI dispersion ($dn_{\text{co}}/d\lambda$). By inscribing five FBGs with different periods in the same fiber as the TFBG, the dispersion of -1.281×10^{-5} nm^{-1} is obtained according to their Bragg wavelengths (1536nm ~ 1568nm). The dispersion value is slightly higher than that of pure silica (-1.198×10^{-5} nm^{-1} at 1550 nm) [22, 23], which can be explained that the germanium doping and UV-exposure in grating fabrication process modified the dispersion characteristics [19]. In order to validate the feasibility of the ERI calibration method for the TFBG, we firstly calculated the ERI (which equals to the RI at the measured wavelength) of the cut-off cladding modes in DI water. The result shows that the RI of water at 1490 nm (@20°C) is 1.3160±0.0012, which is in good agreement with the reported value of 1.3167±0.0004 at 1500 nm by an Abbe refractometer [1]. The calculated ERIs (top-horizontal coordinate) versus the cut-off wavelengths are also shown in Fig. 3(a). As a result, the vernier spectra as a complementary scale can be used to compensate the measurement error caused by the wavelength separation between cladding modes.

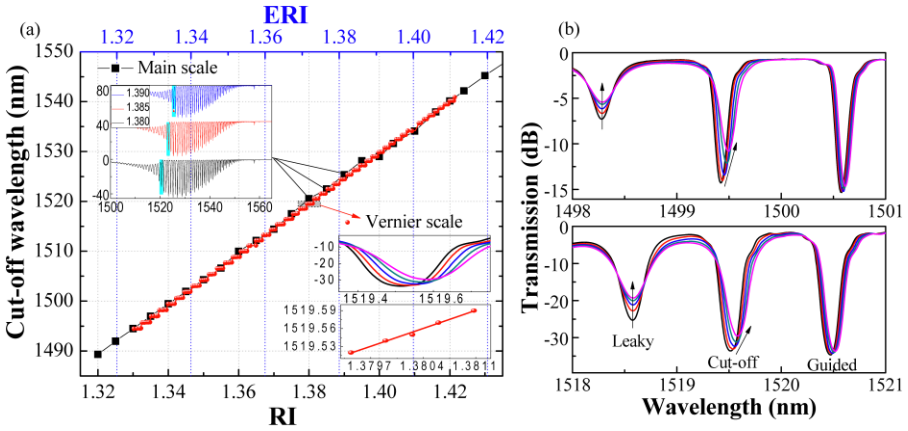

Fig. 3. Calibration relationship of cut-off mode resonant wavelength with the change of surrounding RI. (a) Resonant wavelengths with main scale and vernier scale versus RI (bottom coordinate) and ERI (top coordinate), insets: (top-left) marked wavelength position of the cut-off mode resonances, and (bottom-right) vernier spectra and scale in a zoomed region. (b) Detailed spectral evolutions of the cut-off mode resonances of two different orders in a small RI range.

3.4 Actual application: Temperature dependence of ethanol refractive index

In order to examine the actual application, we experimentally investigated a small RI variation corresponding to a couple of cut-off mode resonances by using the proposed refractometer. Taking the temperature dependence of RI of ethanol as an example, more accurate values of RI at different temperatures are measured. For pre-calibration of temperature induced effects, the TFBG was firstly placed in a heating chamber with a temperature controller, and then we observed the global spectrum red-shift for all the resonances with increasing temperature, showing a positive dn/dT of TFBG itself. The shifts of resonant wavelengths of the core mode and the cladding mode at ~1506 nm are shown in Fig. 4(a), and their temperature sensitivities in air are 10.10 pm/°C and 9.69 pm/°C, respectively. In the experiment, the anhydrous ethanol of high purity (99.99%) was employed, for avoiding the influence of ethanol volatilization on the concentration (and RI) during the heating/cooling process. Based on the ethanol-bath method, the temperature around TFBG was controlled with a heater and monitored with a thermometer. Figure 4(a) shows the measurement results. The core mode has the same temperature response as that in air. However, from Fig. 4(b), the wavelength of cut-off mode resonance changes by ~6nm

towards the shorter wavelength with the temperature rising from 20°C to 50°C, as a result of the dominated negative d*n*/d*T* of alcohol. Taking temperature calibration measured in air into account, and hence, the variation of cut-off wavelength (marked with red circles in Fig. 4(b)) can be used to find the temperature dependence of ethanol RI. It can be seen that after the removal of inherent thermo-optic and thermal expansion effects of TFBG itself, the change of cut-off wavelength is slight larger than original one.

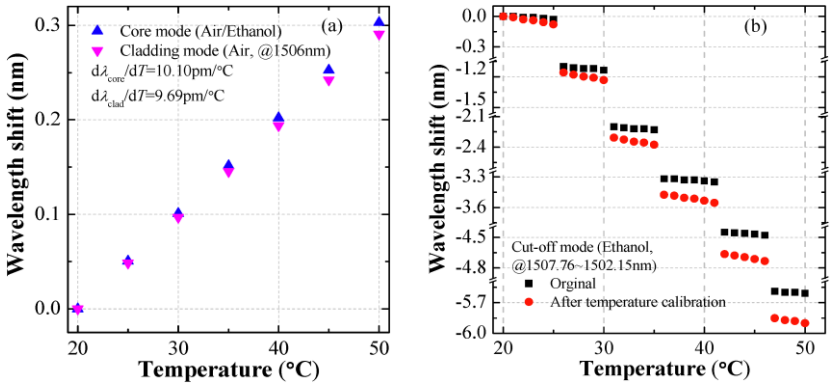

Fig. 4. With the temperature increasing, (a) wavelength shifts of the core and the cladding modes when the TFBG is in air, and (b) wavelength shift of cut-off mode when the TFBG in ethanol.

Finally, the calculated ERI and corresponding RI values at each temperature by the pre-calibration results of the refractometer are plotted in Fig. 5 with solid square/circle symbols. The obtained ERI decreases with increasing temperature, and then the linear fitting curve shows a negative d*n*/d*T* (-4.260×10^{-4}/°C) of ethanol in the temperature range of 20°C~50°C, which is in good agreement with the value of -4.128×10^{-4}/°C calculated from the previous report [24]. And also, the obtained ERI value of ethanol is 1.3510 at 1506nm (@20°C), very close to the reported values of 1.3522 at 1500nm (@20°C) measured by an Abbe refractometer [1] and 1.3503 at 1550nm (@25°C) measured by a large-angle refractometer [25]. The difference between them is mainly introduced by the system error of different calibration approaches and the dispersion of ethanol itself. As a comparison, we only use the main-scale of the refractometer to calculate the ERI (or RI), and the values at each temperature are also plotted in Fig. 5 with half-left up/down-triangle symbol. It is obvious that the ERI/RI does not change continuously with the temperature, and there will be considerable error in measurement, for instance, maximum error 1.87×10^{-3} of the calculated RI at 25°C. On the other hand, using the vernier-scale can overcome the measurement uncertainty caused by the separation of the cut-off cladding modes, as also mentioned in [19].

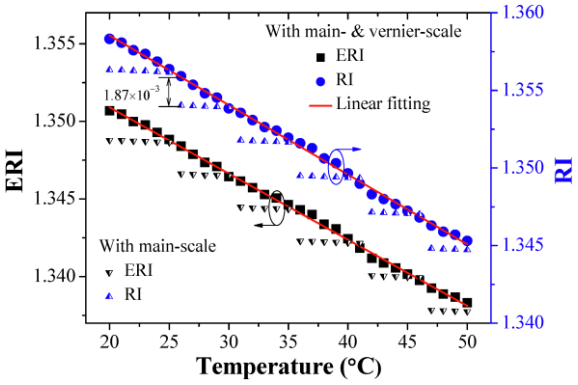

Fig. 5. Variations of the calculated ERI and RI with the temperature.

3.5 Determination of repeatability and uncertainty

To determine the key factors of repeatability and the uncertainty of the proposed TFBG-based refractometer, three sets of measurements for each temperature were carried out. As shown in Fig. 6, the results demonstrate that both of core mode and cut-off mode have a good repeatability under different temperatures, and their maximum wavelength fluctuation is only ±0.005nm, which corresponds to a RI value of $\pm 1.359\times10^{-4}$. This uncertainty value is better than $\pm10^{-3}$ reported in [18] and 1.87×10^{-3} obtained only with the main-scale. It is not as good as the value of $\pm5\times10^{-5}$ reported in [19] due that it is affected by the accuracy of spectral analyzer. However, the proposed "vernier" approach can be implemented as a simpler metering tool when the highest possible accuracy is not needed for the application. Also, from the inset of Fig. 6, it is also evident that the three measurement spectra are almost completely overlapped at 40°C, and a small spectral shift in the interval of 1°C can be observed. In addition, the RI measurement uncertainty is also dependent on wavelength shift of the cut-off mode resonance and the resolution of the spectral measurement instrument.

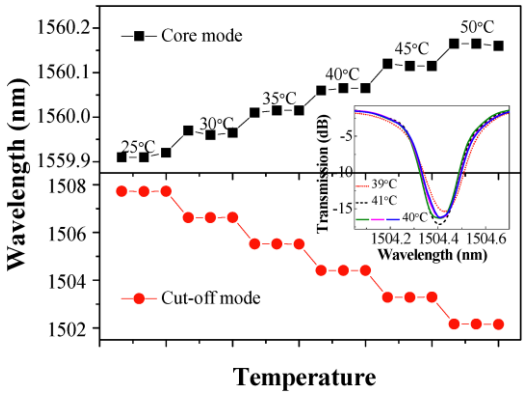

Fig. 6. Determination of repeatability and uncertainty of the refractometer. Inset: the spectra of three measurements at 40°C and the spectral shift in the interval of 1°C.

Although the temperature dependence of the RI of anhydrous ethanol as an example was investigated, for the first time, to demonstrated the metrological performance of the refractometer, the applications should be extended the dynamic and static high-accuracy measurement of absolute RI of liquids. The accuracy could be further improved by using a standard RI liquid sets with smaller interval and more precision spectrum instrument to strictly pre-calibrate the vernier spectra, where the more precise and finer wavelength information would be obtained.

4. Conclusion

We proposed and experimentally demonstrated an optical fiber-based refractometer by using the comb-like spectrum of a TFBG for high-precision RI measurement and temperature-dependence of RI of anhydrous ethanol in the NIR range. Prior to use, the main-scale of the refractometer was pre-calibrated with a series of liquids with known RIs, and the more precise vernier-scale measurement is demonstrated by a series of sucrose solutions with different concentrations. When changing the temperature of liquid, the RI can be discriminately measured with the temperature and RI responses of different modes in air and liquid. The results show that the temperature-dependence of RI of ethanol is -4.260×10^{-4}/°C in the temperature range of 20°C~50°C, and the uncertainty is approximately $\pm1.359\times10^{-4}$ by calculating the three measurement results. The proposed refractometer with temperature-calibration therefore has the merits of enhanced precision, high repeatability, and robust fiber structure, and then can be applied in dynamic and static RI measurement, especially in the measurement of a very small and continuous RI change.

Funding

Marie Skłodowska-Curie Individual Fellowships in the European Union's Horizon 2020 Research and Innovation Programme (660648); National Natural Science Foundation of China (61505165); Natural Science Basic Research Plan in Shaanxi Province of China (2016JQ6032).